

Matrix-analytic solution of infinite, finite and level-dependent second-order fluid models

Gábor Horváth · Miklós Telek

Received: date / Accepted: date

Abstract This paper presents a matrix-analytic solution for second-order Markov fluid models (also known as Markov-modulated Brownian motion) with level-dependent behavior. A set of thresholds is given, that divide the fluid buffer into homogeneous regimes. The generator matrix of the background Markov chain, the fluid rates (drifts) and the variances can be regime dependent.

The model allows the mixing of second-order states (with positive variance) and first-order states (with zero variance) and states with zero drift. The behavior at the upper and lower boundary can be reflecting, absorbing, or the combination of them.

In every regime the solution is expressed as a matrix-exponential combination, whose matrix parameters are given by the minimal non-negative solution of matrix quadratic equations, that can be obtained by any of the well-known solution methods available for quasi birth death processes (QBDs).

The probability masses and the initial vectors of the matrix exponential terms are the solutions of a set of linear equations. However, to have the necessary number of equations, new relations are required for the level boundary behavior, relations that were not needed in first-order level dependent and in homogeneous (non-level-dependent) second-order fluid models.

The presented method can solve systems with hundreds of states and hundreds of thresholds without numerical issues.

G. Horváth
Budapest University of Techn. and Econ., Dept. of Networked Systems and Services
Magyar tudósok krt 2., 1117 Budapest, Hungary
Tel.: +36-1-4633254
E-mail: ghorvath@hit.bme.hu

M. Telek
MTA-BME Information Systems Research Group
Magyar tudósok krt 2., 1117 Budapest, Hungary
Tel.: +36-1-4632084

Keywords Second order Markov fluid queue · Markov-modulated Brownian motion · level dependent behaviour · stationary analysis · matrix analytic solution

Mathematics Subject Classification (2010) 60K25 · 90B22

1 Introduction

First-order Markov fluid models (or simply Markov fluid models) are queueing models where the queue length is continuous and the rate at which the queue length (also referred to as fluid level) changes is modulated by a background continuous time Markov chain (CTMC). These fluid models have been applied successfully in many application areas e.g., [Hohn et al(2004)Hohn, Veitch, Papagiannaki, and Diot, Stanford et al(2005)Stanford, Latouche, Woolford, Boychuk, and Hunchak]. Several solution methods exist to obtain the stationary distribution of the fluid level (eigenvalue decomposition based [Karandikar and Kulkarni(1995)], Schur decomposition based [Akar and Sohraby(2004)], matrix-analytic [Ramaswami(1999), da Silva Soares and Latouche(2006)], invariant subspace [Akar and Sohraby(1997)], etc.). The basic infinite buffer homogeneous model has been extended in several ways, e.g., finite buffer and level-dependent variants, and the associated analytical description and numerical methods also appeared in the literature e.g., [da Silva Soares and Latouche(2009), Bekker et al(2009)Bekker, Boxma, and Resing, Bean and O'Reilly(2008)].

The second-order Markov fluid models (also known as Markov-modulated Brownian motion) can be viewed as an extension as well. In these models the fluid level does not change linearly, but has a Brownian motion component, whose variance can be state dependent. While the first results investigating this system appeared relatively early [Rogers(1994), Asmussen(1995), Karandikar and Kulkarni(1995)], solutions avoiding the numerically demanding eigenvalue decomposition and complex arithmetic by extending the matrix-analytic methods towards second-order models appeared only recently. Results for the stationary analysis of the finite case also exists [Gribaudo et al(2008)Gribaudo, Manini, Sericola, and Telek, Ivanovs(2010), Latouche and Nguyen(2015a)], but for the level-dependent case only transient results are available [Chen et al(2002)Chen, Hong, and Trivedi].

In this paper we consider second-order Markov fluid models with level-dependent behavior for two main reasons. On the one hand, the presence of active queue management [Le et al(2007)Le, Aikat, Jeffay, and Smith] in some telecommunication systems motivate the solution of such models, and on the other hand, the stationary analysis of first-order piecewise constant level dependent fluid models is known, but it is unknown for second order fluid models. The proposed solution follows the matrix-analytic method, the stationary solution is expressed as a matrix-exponential combination in every regime. One of the contributions of the paper is that the computations of the required characteristic matrices are mapped to the

minimal non-negative solutions of matrix quadratic equations, for which well established, quadratically convergent, numerically stable, well-known solution methods are available [Bini et al(2005)Bini, Latouche, and Meini], while previous solution methods were restricted to specific linearly convergent iterative schemes [Breuer(2012)] or spectral decomposition [Karandikar and Kulkarni(1995)] up to very recent superlinear results [Latouche and Nguyen(2015b), Ahn and Ramaswami(2017)]. Based on the characteristic matrices, the missing elements of the stationary solution, the probability masses and the stationary densities at region borders, are obtained as the solutions of a linear system. However, to obtain this linear system, as the second main contribution of the paper, we needed to establish a new relation between the densities below and above the borders of homogeneous regions. This new relation was not considered before, because it is not necessary for the stationary solution of level-independent second-order Markov fluid models [Ivanovs(2010)].

The rest of the paper is organized as follows. Section 2 presents the matrix-analytic solution of simple infinite second-order fluid models. The technique to obtain the matrix parameters of the solution by the analysis of a special QBD is introduced here as well. Section 3 extends the results to the homogeneous finite buffer case. The level-dependent extension is discussed in Section 4, where the new relations characterizing the fluid behavior around the level boundaries are also presented. Finally, Section 5 closes the paper with some numerical examples demonstrating that the presented procedure is able to solve large systems with hundreds of states and hundreds of thresholds as well.

2 Infinite buffer second-order Markov fluid models

Second-order Markov fluid models are two-dimensional processes $\{\mathcal{X}(t), \mathcal{Z}(t), t \geq 0\}$, where $\mathcal{Z}(t)$ is an irreducible background CTMC with generator \mathbf{Q} and state space \mathcal{S} , and $\mathcal{X}(t)$ represents the level of the fluid in a buffer. When the CTMC stays in state i in $(t, t + \Delta)$, the increment of $\mathcal{X}(t)$ is normally distributed with mean $r_i \Delta$ and variance $\sigma_i^2 \Delta$. Diagonal matrices \mathbf{R} and \mathbf{S} contain the drift and variance parameters, hence $\mathbf{R} = \text{diag}(r_i)$ and $\mathbf{S} = \text{diag}(\sigma_i^2/2)$ (the variances are divided by 2 in order to make the arising expressions simpler).

Let us denote the stationary fluid level density by vector $f(x) = [f_i(x), i \in \mathcal{S}]$, defined by $f_i(x) = \lim_{t \rightarrow \infty} \frac{d}{dx} P(\mathcal{X}(t) < x, \mathcal{Z}(t) = i)$. The probability mass accumulating at level 0 and state i is denoted by $p_i = \lim_{t \rightarrow \infty} P(\mathcal{X}(t) = 0, \mathcal{Z}(t) = i)$. $f(x)$ satisfies the differential equation for $x > 0$ [Karandikar and Kulkarni(1995), Eq. (21)]

$$\frac{d}{dx} f(x) \mathbf{R} - \frac{d^2}{dx^2} f(x) \mathbf{S} = f(x) \mathbf{Q}, \quad (1)$$

and the boundary equation [Karandikar and Kulkarni(1995), Eq. (22)]

$$f(0) \mathbf{R} - f'(0) \mathbf{S} = p \mathbf{Q}. \quad (2)$$

The behavior at the boundary in (first-order) Markov fluid models is well defined: a probability mass can accumulate in states with non-positive rate, while the mass is zero in states with positive rates. In the second-order case, however, two different boundary behaviors are distinguished in the literature, the *reflecting* [Cox and Miller(1972), Section 5.7.ii], and the *absorbing* boundary [Cox and Miller(1972), Section 5.7.i].

- If state i with $\sigma_i > 0$ (also referred to as second-order state) is *reflecting* at the boundary then the probability mass is zero in state i (that is $p_i = 0$).
- If a second-order state i is *absorbing* at the boundary then probability mass can accumulate ($p_i > 0$) but the density at level 0 is zero ($f_i(0) = 0$).

The state space \mathcal{S} is partitioned according to the sign of the rates and variances as follows:

- $\mathcal{S}^+ = \{i \in \mathcal{S} : r_i > 0, \sigma_i^2 = 0\}$,
- $\mathcal{S}^- = \{i \in \mathcal{S} : r_i < 0, \sigma_i^2 = 0\}$,
- $\mathcal{S}^0 = \{i \in \mathcal{S} : r_i = 0, \sigma_i^2 = 0\}$,
- $\mathcal{S}^{\sigma+} = \{i \in \mathcal{S} : r_i > 0, \sigma_i^2 > 0\}$,
- $\mathcal{S}^{\sigma-} = \{i \in \mathcal{S} : r_i < 0, \sigma_i^2 > 0\}$,
- $\mathcal{S}^{\sigma 0} = \{i \in \mathcal{S} : r_i = 0, \sigma_i^2 > 0\}$,

and $\mathcal{S}^\sigma = \mathcal{S}^{\sigma+} \cup \mathcal{S}^{\sigma-} \cup \mathcal{S}^{\sigma 0}$ gathers the second-order states. Hence, we have that $\mathcal{S} = \mathcal{S}^+ \cup \mathcal{S}^\sigma \cup \mathcal{S}^- \cup \mathcal{S}^0$ and without loss of generality we assume that the states are ordered according to this subset partitioning. To avoid degenerate cases we assume that $\mathcal{S}^+ \cup \mathcal{S}^{\sigma+} \neq \emptyset$ and $\mathcal{S}^- \cup \mathcal{S}^{\sigma-} \neq \emptyset$.

2.1 The stationary solution

First we establish the relation between the stationary behavior in the zero states, $i \in \mathcal{S}^0$ and the rest of the state space $\mathcal{S}^* = \mathcal{S} \setminus \mathcal{S}^0$. With the given state ordering the generator has a block structure

$$\mathbf{Q} = \begin{bmatrix} \mathbf{Q}_{**} & \mathbf{Q}_{*0} \\ \mathbf{Q}_{0*} & \mathbf{Q}_{00} \end{bmatrix}, \quad (3)$$

by which differential equation (1) can be partitioned to

$$f_0(x) = f_*(x) \mathbf{Q}_{*0} (-\mathbf{Q}_{00})^{-1}, \quad (4)$$

$$\frac{d}{dx} \underbrace{f_*(x)}_{\bar{f}(x)} \underbrace{\mathbf{R}_*}_{\bar{\mathbf{R}}} - \frac{d^2}{dx^2} \underbrace{f_*(x)}_{\bar{f}(x)} \underbrace{\mathbf{S}_*}_{\bar{\mathbf{S}}} = \underbrace{f_*(x)}_{\bar{f}(x)} \underbrace{(\mathbf{Q}_{**} + \mathbf{Q}_{*0} (-\mathbf{Q}_{00})^{-1} \mathbf{Q}_{0*})}_{\bar{\mathbf{Q}}}. \quad (5)$$

As reflected by (5) and the introduced notations with upper bar, the differential equation governing the restricted system with the zero rates censored out are similar to (1). Knowing $\bar{f}(x)$, the density of the original (non-censored) system can be recovered by

$$f(x) = [\bar{f}(x) f_0(x)] = \bar{f}(x) \underbrace{[\mathbf{I} \quad \mathbf{Q}_{*0} (-\mathbf{Q}_{00})^{-1}]}_{\mathbf{Z}}, \quad (6)$$

where the size of \mathbf{Z} is $|\mathcal{S}^*| \times |\mathcal{S}|$.

In the rest of the section we focus on the solution of (5). It is assumed that in the restricted system the ordering of the states is $\mathcal{S}^+, \mathcal{S}^{\sigma^+}, \mathcal{S}^{\sigma_0}, \mathcal{S}^{\sigma^-}, \mathcal{S}^-$.

From e.g. [Ivanovs(2010)], it is known that $\bar{f}(x)$ can be expressed in a matrix-exponential form, where the order of the matrix-exponential equals $|\mathcal{S}^\bullet|$ with $\mathcal{S}^\bullet = \mathcal{S}^+ \cup \mathcal{S}^\sigma$ [Karandikar and Kulkarni(1995), Theorem 4.]. Thus, the solution can be transformed into the following form

$$\bar{f}(x) = \pi e^{\mathbf{K}x} [\mathbf{I} \quad \mathbf{\Psi}], \quad (7)$$

where the size of \mathbf{K} is $|\mathcal{S}^\bullet| \times |\mathcal{S}^\bullet|$ and the size of $\mathbf{\Psi}$ is $|\mathcal{S}^\bullet| \times |\mathcal{S}^-|$. The form of the solution is the same as in first order fluid models, therefore we used the same notations for the matrices. It is important to note, however, that matrices \mathbf{K} and $\mathbf{\Psi}$ do not have the same elegant probabilistic interpretations as they have in [Ramaswami(1999)] for the first order case.

In order to fully characterize the stationary behavior, it remains to obtain

- matrices \mathbf{K} and $\mathbf{\Psi}$,
- vector π ,
- and the vector of probability masses at level 0 p .

2.2 Computing matrices \mathbf{K} and $\mathbf{\Psi}$

Substituting the solution (7) into the differential equation (5) gives

$$\mathbf{K}\bar{\mathbf{R}}_\bullet - \mathbf{K}^2\bar{\mathbf{S}}_\bullet = \bar{\mathbf{Q}}_{\bullet\bullet} + \mathbf{\Psi}\bar{\mathbf{Q}}_{-\bullet}, \quad (8)$$

$$\mathbf{K}\mathbf{\Psi}\bar{\mathbf{R}}_- - \underbrace{\mathbf{K}^2\mathbf{\Psi}\bar{\mathbf{S}}_-}_0 = \bar{\mathbf{Q}}_{\bullet-} + \mathbf{\Psi}\bar{\mathbf{Q}}_{--}, \quad (9)$$

where $\bar{\mathbf{S}}_- = \mathbf{0}$ has been exploited.

In the first-order case, when $\mathcal{S}^\sigma = \emptyset$, equations (8) and (9) are easy to solve: expressing \mathbf{K} from (8) and inserting the result into (9) leads to the well-known matrix Riccati equation for matrix $\mathbf{\Psi}$. In the second-order case, however, $\mathbf{\Psi}$ and \mathbf{K} can not be obtained this way. Instead, a special QBD Markov chain is introduced, and the fundamental matrix of this QBD will provide matrices $\mathbf{\Psi}$ and \mathbf{K} .

The regular part of the block-tri-diagonal generator of QBDs are characterized by three matrices: the transition rates corresponding to level-forward (\mathbf{F}), local (\mathbf{L}) and level-backward (\mathbf{B}) transitions. In our case, these matrices are defined as

$$\begin{aligned} \mathbf{F} &= \begin{bmatrix} \frac{1}{c}\bar{\mathbf{Q}}_{\bullet\bullet} + \bar{\mathbf{R}}_\bullet + c\bar{\mathbf{S}}_\bullet & \frac{1}{c}\bar{\mathbf{Q}}_{\bullet-} \\ \mathbf{0} & \mathbf{0} \end{bmatrix}, \\ \mathbf{L} &= \begin{bmatrix} -\bar{\mathbf{R}}_\bullet - 2c\bar{\mathbf{S}}_\bullet & \mathbf{0} \\ \frac{1}{c}\bar{\mathbf{Q}}_{-\bullet} & \frac{1}{c}\bar{\mathbf{Q}}_{--} + \bar{\mathbf{R}}_- \end{bmatrix}, \\ \mathbf{B} &= \begin{bmatrix} c\bar{\mathbf{S}}_\bullet & \mathbf{0} \\ \mathbf{0} & -\bar{\mathbf{R}}_- \end{bmatrix}, \end{aligned} \quad (10)$$

where c is an arbitrary constant such that

$$c > \max \left(1, \max_{i \in \mathcal{S}^+} \frac{|\bar{q}_{ii}|}{\bar{r}_i}, \max_{i \in \mathcal{S}^\sigma} \frac{1}{2\bar{s}_i} (\sqrt{\bar{r}_i^2 + 4\bar{s}_i|\bar{q}_{ii}|} - \bar{r}_i) \right). \quad (11)$$

When the variance is positive in all states, $\mathcal{S}^\sigma = \mathcal{S}$ and $\mathcal{S}^+ = \mathcal{S}^- = \emptyset$, then \mathbf{F} , \mathbf{L} and \mathbf{B} reduces to the upper left blocks in (10).

Observe that these matrices define a proper QBD, since due to (11)

$$\frac{1}{c} \bar{\mathbf{Q}}_{++} + \bar{\mathbf{R}}_+ > 0, \quad (12)$$

$$\frac{1}{c} \bar{\mathbf{Q}}_{\sigma\sigma} + \bar{\mathbf{R}}_\sigma + c\bar{\mathbf{S}}_\sigma > 0, \quad (13)$$

hold, hence $\frac{1}{c} \bar{\mathbf{Q}}_{\bullet\bullet} + \bar{\mathbf{R}}_\bullet + c\bar{\mathbf{S}}_\bullet$ (and therefore \mathbf{F}) is non-negative. Furthermore, due to (11), $-\bar{\mathbf{R}}_{\sigma-} - 2c\bar{\mathbf{S}}_{\sigma-} < 0$ holds, hence $-\bar{\mathbf{R}}_\bullet - 2c\bar{\mathbf{S}}_\bullet$ (and therefore \mathbf{L}) is a valid sub-generator. The non-negativity of \mathbf{B} is straightforward. It can be checked that the row-sum of $\mathbf{F} + \mathbf{L} + \mathbf{B}$ is zero as well.

Let $\mathbf{1}$ denote the column vector of ones of appropriate size. The condition of stability of the fluid system is, $\alpha \bar{\mathbf{R}} \mathbf{1} < 0$, where $\alpha \bar{\mathbf{Q}} = 0$ and $\alpha \mathbf{1} = 1$. In the rest of the section we assume stable (positive recurrent) infinite buffer system. The condition of stability of the QBD is, $\gamma \mathbf{B} \mathbf{1} > \gamma \mathbf{F} \mathbf{1}$, where $\gamma(\mathbf{B} + \mathbf{L} + \mathbf{F}) = 0$ and $\gamma \mathbf{1} = 1$.

Lemma 1 *The fluid system is positive recurrent iff the QBD is positive recurrent.*

Proof $\alpha = \gamma$, because $\mathbf{B} + \mathbf{L} + \mathbf{F} = \bar{\mathbf{Q}}/c$. Using $\bar{\mathbf{Q}}_{\bullet\bullet} \mathbf{1} + \bar{\mathbf{Q}}_{\bullet-} \mathbf{1} = 0$, $\gamma \mathbf{B} \mathbf{1} > \gamma \mathbf{F} \mathbf{1}$ simplifies to $\gamma_\bullet \bar{\mathbf{R}}_\bullet \mathbf{1} + \gamma_- \bar{\mathbf{R}}_- \mathbf{1} < 0$, which is identical with $\alpha \bar{\mathbf{R}} \mathbf{1} < 0$.

Theorem 1 *The minimal non-negative solution of the matrix-quadratic equation $\mathbf{F} + \mathbf{R}\mathbf{L} + \mathbf{R}^2\mathbf{B} = \mathbf{0}$ is*

$$\mathbf{R} = \begin{bmatrix} \frac{1}{c} \mathbf{K} + \mathbf{I} & \Psi \\ \mathbf{0} & \mathbf{0} \end{bmatrix}. \quad (14)$$

Proof Substituting the solution gives identity for the matrix equations (8), (9). Due to the stability of the QBD, the eigenvalues of \mathbf{R} are in the open unit disc. The eigenvalues of $\frac{1}{c} \mathbf{K}$ are obtained from the eigenvalues of \mathbf{R} shifted to the left by one. As a result the eigenvalues of $\frac{1}{c} \mathbf{K}$ as well as the eigenvalues of \mathbf{K} have negative real part. According to [Karandikar and Kulkarni(1995)] the number of eigenvalues which contribute to the matrix exponential solution is $|\mathcal{S}^\bullet|$, which equals the size of \mathbf{K} .

As a consequence of the stability condition, \mathbf{K} is invertible, because the real part of its eigenvalues are strictly negative.

2.3 Computing vectors π and p

To fully characterize the stationary behavior, it remains to compute the length $|\mathcal{S}|$ vector p and the length $|\mathcal{S}^\bullet|$ vector π based on the behavior around level 0. Let us partition the second-order states into two sub-sets, $\mathcal{S}^\sigma = \mathcal{S}^A \cup \mathcal{S}^R$, depending on the boundary behavior. If the fluid level hits 0 in \mathcal{S}^A , the behavior is absorbing, which means that the level remains 0 till the background process changes state. In states \mathcal{S}^R , however, the boundary is reflecting, when the Brownian motion would go below 0, it is reflected to the positive domain.

To obtain the p and π parameters a set of linear equations is created as follows.

- $|\mathcal{S}|$ equations are given by (2), hence

$$\underbrace{\pi [\mathbf{I} \ \Psi] \mathbf{Z} \mathbf{R}}_{f(0)} - \underbrace{\pi \mathbf{K} [\mathbf{I} \ \Psi] \mathbf{Z} \mathbf{S}}_{f'(0)} = p \mathbf{Q}, \quad (15)$$

where matrix \mathbf{Z} is introduced by (6).

- $|\mathcal{S}^+|$ equations express that the probability mass is zero in the positive states,

$$p_i = 0, \quad \text{for } i \in \mathcal{S}^+. \quad (16)$$

- $|\mathcal{S}^R|$ equations express that the probability mass is zero in second-order states with reflecting boundary behavior,

$$p_i = 0, \quad \text{for } i \in \mathcal{S}^R. \quad (17)$$

- $|\mathcal{S}^A|$ equations express that the density at the boundary is zero in second-order states with absorbing boundary, thus

$$(\pi [\mathbf{I} \ \Psi] \mathbf{Z}) e_i = 0, \quad \text{for } i \in \mathcal{S}^A, \quad (18)$$

where e_i is the i th unit column vector whose only non-zero element is 1 at position i .

The number of these equations matches the number of unknowns.

The obtained linear set of equations, (15)-(18), is either full rank and $\pi = 0$ and $p = 0$ is its only solution or rank deficient. In the later case, the additional normalizing equation

$$p \mathbf{1} + \int_0^\infty f(x) dx \mathbf{1} = p \mathbf{1} + \pi (-\mathbf{K})^{-1} [\mathbf{I} \ \Psi] \mathbf{Z} \mathbf{1} = 1, \quad (19)$$

makes the linear system full rank in case of single rank deficit (which is commonly assumed for non-degenerate systems [Karandikar and Kulkarni(1995)]).

3 Finite buffer second-order Markov fluid models

The finite buffer variant of second-order Markov fluid model is defined in the same way as the infinite buffer one and the only difference is that the fluid level is upper bounded at level B . Between the boundaries the fluid level still evolves according to the differential equation (1), however, besides equation (2), which is still valid around level 0, a similar relation holds for the upper boundary [Karandikar and Kulkarni(1995)]

$$-f(B)\mathbf{R} + f'(B)\mathbf{S} = f(B)\mathbf{Q}. \quad (20)$$

3.1 Stationary solution

The states in \mathcal{S}^0 can be treated as in Section 2.1, hence we focus on the solution of $\bar{f}(x)$, for $x \in [0, B]$ in the sequel.

Just like in the first-order case, in the presence of an upper boundary the stationary distribution is a matrix-exponential combination [Ivanovs(2010)], that can be transformed to

$$\bar{f}(x) = \pi_f e^{\mathbf{K}_f x} [\mathbf{I} \ \Psi_f] + \pi_b e^{\mathbf{K}_b (B-x)} [\Psi_b \ \mathbf{I}], \quad (21)$$

which consists of a *forward* and a *backward* term denoted by subscript f and b , respectively. The order of the forward matrix-exponential term is $|\mathcal{S}^+| + |\mathcal{S}^\sigma|$ and the order of the backward one is $|\mathcal{S}^-| + |\mathcal{S}^\sigma|$.

The parameters of the forward term can be determined as before: a QBD is constructed based on the $\bar{\mathbf{Q}}$, $\bar{\mathbf{R}}$ and $\bar{\mathbf{S}}$ parameters according to (10), then matrices \mathbf{K}_f and Ψ_f can be extracted from the fundamental matrix of the QBD. To obtain the matrices of the backward term, \mathbf{K}_b and Ψ_b , the same procedure has to be applied with $\bar{\mathbf{Q}}$, $-\bar{\mathbf{R}}$ and $\bar{\mathbf{S}}$ as input, since in the level reverse process, $-\bar{\mathbf{R}}$ must be used instead of $\bar{\mathbf{R}}$. Note that, \mathcal{S}^+ becomes “ \mathcal{S}^- ” in the level reverse process and consequently the c constants can be different for the forward and backward cases.

The eigenvalues of both \mathbf{K}_f and \mathbf{K}_b are non-positive, however, depending on the mean drift, one of them has a zero eigenvalue. In case of positive drift, \mathbf{K}_f has the zero eigenvalue, hence it can not be inverted; in case of negative drift, it is matrix \mathbf{K}_b that does not have an inverse. We neglect the zero drift case for simplicity noting that the computation of \mathbf{K}_f and \mathbf{K}_b does not cause any special difficulty in that case, but the solution of the obtained linear system needs special treatment [Telek and Vécsei(2012)].

3.2 Obtaining the boundary vectors

The stationary distribution depends on four parameters in the finite buffer case. Size $|\mathcal{S}|$ row vectors $p^{(0)}$ and $p^{(B)}$ are the probability masses at level 0 and level B , respectively. The initial vectors of the matrix-exponential terms are

π_f and π_b , with length $|\mathcal{S}^+| + |\mathcal{S}^\sigma|$ and $|\mathcal{S}^-| + |\mathcal{S}^\sigma|$, respectively. Consequently, the total number of unknowns corresponding to the boundaries are $3|\mathcal{S}| + |\mathcal{S}^\sigma|$.

If the second order states are partitioned according to the behavior at the lower boundary as $\mathcal{S}^\sigma = \mathcal{S}^{A_0} \cup \mathcal{S}^{R_0}$ and at the upper boundary as $\mathcal{S}^\sigma = \mathcal{S}^{A_B} \cup \mathcal{S}^{R_B}$, the equations for the unknowns are

- $|\mathcal{S}|$ equations for the lower boundary, given by (2),

$$\begin{aligned} & \underbrace{(\pi_f [\mathbf{I} \ \Psi_f] + \pi_b e^{\mathbf{K}_b B} [\Psi_b \mathbf{I}]) \mathbf{Z} \mathbf{R}}_{f(0)} \\ & - \underbrace{(\pi_f \mathbf{K}_f [\mathbf{I} \ \Psi_f] - \pi_b \mathbf{K}_b e^{\mathbf{K}_b B} [\Psi_b \mathbf{I}]) \mathbf{Z} \mathbf{S}}_{f'(0)} = p^{(0)} \mathbf{Q}. \end{aligned} \quad (22)$$

- $|\mathcal{S}|$ equations for the upper boundary, given by (20),

$$\begin{aligned} & - \underbrace{(\pi_f e^{\mathbf{K}_f B} [\mathbf{I} \ \Psi_f] + \pi_b [\Psi_b \mathbf{I}]) \mathbf{Z} \mathbf{R}}_{f(B)} \\ & + \underbrace{(\pi_f \mathbf{K}_f e^{\mathbf{K}_f B} [\mathbf{I} \ \Psi_f] - \pi_b \mathbf{K}_b [\Psi_b \mathbf{I}]) \mathbf{Z} \mathbf{S}}_{f'(B)} = p^{(B)} \mathbf{Q}. \end{aligned} \quad (23)$$

- $|\mathcal{S}^+| + |\mathcal{S}^{R_0}|$ equations expressing that the mass is zero at the lower boundary

$$p_i^{(0)} = 0, \quad \text{for } i \in \mathcal{S}^+ \cup \mathcal{S}^{R_0}. \quad (24)$$

- $|\mathcal{S}^-| + |\mathcal{S}^{R_B}|$ equations expressing that the mass is zero at the upper boundary

$$p_i^{(B)} = 0, \quad \text{for } i \in \mathcal{S}^- \cup \mathcal{S}^{R_B}. \quad (25)$$

- $|\mathcal{S}^{A_0}|$ equations for zero density in absorbing states at the lower boundary

$$((\pi_f [\mathbf{I} \ \Psi_f] + \pi_b e^{\mathbf{K}_b B} [\Psi_b \mathbf{I}]) \mathbf{Z}) e_i = 0, \quad \text{for } i \in \mathcal{S}^{A_0}. \quad (26)$$

- $|\mathcal{S}^{A_B}|$ equations for zero density in absorbing states at the upper boundary

$$((\pi_f e^{\mathbf{K}_f B} [\mathbf{I} \ \Psi_f] + \pi_b [\Psi_b \mathbf{I}]) \mathbf{Z}) e_i = 0, \quad \text{for } i \in \mathcal{S}^{A_B}. \quad (27)$$

The total number of linear equations is $3|\mathcal{S}| + |\mathcal{S}^\sigma|$, matching the number of unknowns.

Similar to the infinite case, the normalization condition,

$$p^{(0)} \mathbf{1} + \pi_f \int_0^B e^{\mathbf{K}_f x} dx [\mathbf{I} \ \Psi_f] \mathbf{Z} \mathbf{1} + \pi_b \int_0^B e^{\mathbf{K}_b x} dx [\Psi_b \mathbf{I}] \mathbf{Z} \mathbf{1} + p^{(B)} \mathbf{1} = 1,$$

where we used that $\int_0^B e^{\mathbf{K}_b x} dx = \int_0^B e^{\mathbf{K}_b(B-x)} dx$, is necessary to make the system full rank.

In the finite case, however, care has to be taken when evaluating the integrals. As mentioned earlier, either \mathbf{K}_f or \mathbf{K}_b can not be inverted, depending on the mean drift. If we assume that \mathbf{K}_b can not be inverted (that occurs when the mean drift is negative) and the left- and right eigenvectors corresponding to the zero eigenvalue are denoted by ℓ and r (and are normalized such that $\ell \cdot r = 1$), the closed form solution for the integral is

$$\int_0^B e^{\mathbf{K}_b x} dx = (-\mathbf{K}_b + r \cdot \ell)^{-1} (\mathbf{I} - e^{\mathbf{K}_b B}) + B r \cdot \ell. \quad (28)$$

4 Level-dependent second-order fluid models

In the level-dependent system there is a set of thresholds $T_k, k = 0, \dots, K$, with $T_0 = 0$ and $T_K = B$. These $K + 1$ thresholds divide the fluid buffer into K regimes. The system parameters are constant in each regime. **The existence and the uniqueness of this model is provided by [Bass and Pardoux(1987), Stroock and Varadhan(2007)] for the case when $\sigma_i^{(k)} > 0$ ($\forall i \in \mathcal{S}, \forall k \in \{0, \dots, K\}$) and by [Cox and Miller(1972), Section 5.7.ii] and [Cox and Miller(1972), Section 5.7.i] for the lower and upper buffer limit with *reflecting* and *absorbing* boundary behaviour, respectively. The case when $\sigma_i^{(k)} > 0$ and $\sigma_i^{(k+1)} = 0$ behaves as if T_k^- was an upper boundary of the process in region k with *reflecting* or *absorbing* boundary, which is a model parameter similar to the boundary behaviour at the lower and upper buffer limit.** If the fluid level falls into regime k , thus $\mathcal{X}(t) \in (T_{k-1}, T_k)$, the evolution of the process is governed by generator $\mathbf{Q}^{(k)}$, drift matrix $\mathbf{R}^{(k)}$ and variance matrix $\mathbf{S}^{(k)}$, with state groups $\mathcal{S}^{+(k)}, \mathcal{S}^{-(k)}, \mathcal{S}^{0(k)}, \mathcal{S}^{\sigma^{+(k)}}, \mathcal{S}^{\sigma^{-(k)}}, \mathcal{S}^{\sigma_0^{(k)}}$, for $k = 1, \dots, K$. To avoid degenerate cases we assume that $\mathbf{Q}^{(k)}$ is irreducible, $\mathcal{S}^{+(k)} \cup \mathcal{S}^{\sigma^{+(k)}} \neq \emptyset$, $\mathcal{S}^{-(k)} \cup \mathcal{S}^{\sigma^{-(k)}} \neq \emptyset$ and the mean drift in regime k is non-zero for $k = 1, \dots, K$. In regime k , $x \in (T_{k-1}, T_k)$, the stationary density of the fluid level satisfies the differential equation

$$\frac{d}{dx} f^{(k)}(x) \mathbf{R}^{(k)} - \frac{d^2}{dx^2} f^{(k)}(x) \mathbf{S}^{(k)} = f^{(k)}(x) \mathbf{Q}^{(k)}. \quad (29)$$

According to [Chen et al(2002)Chen, Hong, and Trivedi, Sec. 3], for the regime boundaries we have that

$$p^{(k)} \tilde{\mathbf{Q}}^{(k)} = \begin{cases} f^{(1)}(0+) \mathbf{R}^{(1)} - f^{(1)}(0+) \mathbf{S}^{(1)} & \text{if } k = 0, \\ \begin{aligned} & f^{(k+1)}(T_k+) \mathbf{R}^{(k+1)} - f^{(k+1)}(T_k+) \mathbf{S}^{(k+1)} \\ & - f^{(k)}(T_k-) \mathbf{R}^{(k)} + f^{(k)}(T_k-) \mathbf{S}^{(k)} \end{aligned} & \text{if } 0 < k < K, \\ -f^{(K)}(B-) \mathbf{R}^{(K)} + f^{(K)}(B-) \mathbf{S}^{(K)} & \text{if } k = K, \end{cases} \quad (30)$$

holds. Matrices $\tilde{\mathbf{Q}}^{(k)}, k = 0, \dots, K$ are the generators of the background process right at the thresholds. According to the left hand side of (30), the $\tilde{\mathbf{Q}}^{(k)}$

matrices play role in the stationary behaviour only when probability mass develops at T_k .

Figure 1 presents possible combinations of the fluid rates below and above an internal threshold ($T_k, k = 1, \dots, K - 1$). There are some combinations of fluid rates that are ambiguous (marked with gray background in Figure 1). These cases are called repulsive in the literature and they can be treated by defining fluid rates right on the threshold to decide how the fluid buffer behaves when two contradicting directions are assigned below and above the threshold (see e.g. [Gribaudo et al(2008)Gribaudo, Manini, Sericola, and Telek]). In this paper, however, for notional simplicity we exclude such situations.

4.1 Stationary solution

The treatment of states in \mathcal{S}^0 is the same as in Section 2.1. However, it has to be applied in each regime separately as the set of zero states can be different. As a consequence, matrix $\mathbf{Z}^{(k)}$ introduced by (6) to recover the full density vector from the one censored to non-zero states, is also regime dependent.

Like in case of the level dependent first-order fluid models, the density vector is a piece-wise matrix-exponential combination, thus, for regime k we have that

$$\bar{f}^{(k)}(x) = \pi_f^{(k)} e^{\mathbf{K}_f^{(k)}(x-T_{k-1})} [\mathbf{I} \Psi_f^{(k)}] + \pi_b^{(k)} e^{\mathbf{K}_b^{(k)}(T_k-T_{k-1}-x)} [\Psi_b^{(k)} \mathbf{I}], \quad (31)$$

where the matrices $\mathbf{K}_f^{(k)}, \mathbf{K}_b^{(k)}, \Psi_f^{(k)}$ and $\Psi_b^{(k)}$ are obtained for each regime separately by solving the corresponding QBD for the level forward and the level reversed processes, respectively.

In each regime, at least one of $\mathbf{K}_f^{(k)}$ or $\mathbf{K}_b^{(k)}$ has a zero eigenvalue, hence is not invertible, and needs to be handled according to (28).

4.2 The boundary equations at the thresholds

The real challenge in the analysis of level-dependent second-order fluid models is the solution of the missing parameters, $p^{(k)}$ for $k = 0, \dots, K$, and $\pi_f^{(k)}, \pi_b^{(k)}$ for $k = 1, \dots, K$. The total number of unknowns is $(K+1)|\mathcal{S}| + \sum_{k=1}^K |\mathcal{S}^{+(k)}| + \sum_{k=1}^K |\mathcal{S}^{-(k)}| + 2 \sum_{k=1}^K |\mathcal{S}^{\sigma(k)}|$. For finding the required number of equations we need to introduce new relations, which were not necessary in the analysis of the homogeneous infinite and finite cases discussed before. The required new relation is provided by the next theorem.

Theorem 2 *If the variance associated with state i is positive both below and above internal threshold T_k , it holds that*

$$f_i^{(k)}(T_k-) \sqrt{s_i^{(k)}} = f_i^{(k+1)}(T_k+) \sqrt{s_i^{(k+1)}}, \quad \forall i \in \mathcal{S}^{\sigma(k)} \cap \mathcal{S}^{\sigma(k+1)}. \quad (32)$$

An intuitive explanation of the theorem is as follows. Consider a Brownian particle with rate μ and variance σ^2 . In $(0, t)$, the displacement of the particle due to the rate is proportional with $|\mu|t$ and the displacement due to the variance is proportional with $\sigma\sqrt{t}$. Additionally, state transition of the modulating Markov chain with rate λ occurs with probability λt . Consequently, for small t the variance term, which is proportional with \sqrt{t} , dominates the behaviour and the other terms, which are proportional with t , vanish. Considering boundary T_k with $r_i^{(k)} = r_i^{(k+1)} = 0$, $\tilde{Q}_{ii}^{(k)} = 0$, $\sigma_i^{(k)} = \sigma_i^{(k+1)} = \sigma$ we have a regular Brownian motion around T_k , with $f_i^{(k)}(T_k-) = f_i^{(k+1)}(T_k+)$. If we rescale the axes above T_k by c then for the rescaled system we get $\sigma_i^{(k)} = c\sigma_i^{(k+1)}$ and $f_i^{(k)}(T_k-) = cf_i^{(k+1)}(T_k+)$.

Below we prove the theorem by the convergence of properly defined first order fluid models to a second order one.

Proof The proof is based on the convergence of the associated flip-flop queue to the level dependent Markov modulated Brownian motion. Flip-flop queues have been studied in [Latouche and Nguyen(2015b), Latouche and Nguyen(2015a)]. Flip-flop queues are ordinary (first-order) fluid queues with generator and fluid rate matrices given by

$$\mathbf{T} = \begin{bmatrix} \mathbf{Q} - (1/\epsilon^2)\mathbf{I} & (1/\epsilon^2)\mathbf{I} \\ (1/\epsilon^2)\mathbf{I} & \mathbf{Q} - (1/\epsilon^2)\mathbf{I} \end{bmatrix}, \quad \mathbf{C} = \begin{bmatrix} \mathbf{R} + \sqrt{2\mathbf{S}}/\epsilon & \\ & \mathbf{R} - \sqrt{2\mathbf{S}}/\epsilon \end{bmatrix}. \quad (33)$$

The flip-flop queue converges weakly to a second-order fluid model with parameters \mathbf{Q} , \mathbf{R} and \mathbf{S} as $\epsilon \rightarrow 0$. Let the stationary density function of the flip flop queue be $g_\epsilon(x)$, which, due to the block structure of the parameters consists of two parts, $g_\epsilon(x) = [\hat{g}_\epsilon(x) \check{g}_\epsilon(x)]$. The sum of the two parts provide the density function of the second-order fluid model, that is $\lim_{\epsilon \rightarrow 0} \hat{g}_\epsilon(x) + \check{g}_\epsilon(x) = f(x)$.

The difference between $\hat{g}_\epsilon(x)$ and $\check{g}_\epsilon(x)$ can be derived using the formulas (16), (17), (20), (45) and (46) available in [Latouche and Nguyen(2015b)], leading to

$$\lim_{\epsilon \rightarrow 0} \frac{\hat{g}_\epsilon(x) - \check{g}_\epsilon(x)}{\epsilon} = -\frac{1}{\sqrt{2}} f'(x) \sqrt{\mathbf{S}}. \quad (34)$$

Let us now investigate how the flip-flop queue, and, in limit, the Markov-modulated Brownian motion behaves when its drift and variance changes when crossing the threshold at T_k . Since flip-flop queues are first-order fluid models, their behavior is characterized by

$$g_\epsilon^{(k)}(T_k-) \mathbf{C}^{(k)} - g_\epsilon^{(k+1)}(T_k+) \mathbf{C}^{(k+1)} = 0,$$

which is the special case of the boundary equation (30) with $\mathbf{S}^{(k)} = \mathbf{S}^{(k+1)} = 0$, such that $g_\epsilon^{(k)}(x)$ is the density and $\mathbf{C}^{(k)}$ is the rate matrix. The right hand side of this boundary equation is zero because no probability mass is accumulated at the threshold due to the strictly positive and negative rates in the first and

second set of states (with sufficiently small ϵ), respectively. Based on the block structure of \mathbf{C} we have

$$0 = \begin{bmatrix} \hat{g}_\epsilon^{(k)}(T_{k-}) & \check{g}_\epsilon^{(k)}(T_{k-}) \end{bmatrix} \begin{bmatrix} \mathbf{R}^{(k)} + \sqrt{2\mathbf{S}^{(k)}}/\epsilon \\ \mathbf{R}^{(k)} - \sqrt{2\mathbf{S}^{(k)}}/\epsilon \end{bmatrix} \\ - \begin{bmatrix} \hat{g}_\epsilon^{(k+1)}(T_{k+}) & \check{g}_\epsilon^{(k+1)}(T_{k+}) \end{bmatrix} \begin{bmatrix} \mathbf{R}^{(k+1)} + \sqrt{2\mathbf{S}^{(k+1)}}/\epsilon \\ \mathbf{R}^{(k+1)} - \sqrt{2\mathbf{S}^{(k+1)}}/\epsilon \end{bmatrix}, \quad (35)$$

that defines two equations for $\hat{g}_\epsilon(x)$ and $\check{g}_\epsilon(x)$. Summing the two equations and taking the limit $\epsilon \rightarrow 0$ we get

$$0 = \underbrace{\lim_{\epsilon \rightarrow 0} (\hat{g}_\epsilon^{(k)}(T_{k-}) + \check{g}_\epsilon^{(k)}(T_{k-}))}_{f^{(k)}(T_{k-})} \mathbf{R}^{(k)} + \underbrace{\lim_{\epsilon \rightarrow 0} \frac{1}{\epsilon} (\hat{g}_\epsilon^{(k)}(T_{k-}) - \check{g}_\epsilon^{(k)}(T_{k-}))}_{-f'(k)(T_{k-})\sqrt{\mathbf{S}^{(k)}/2}} \sqrt{2\mathbf{S}^{(k)}} \\ - \underbrace{\lim_{\epsilon \rightarrow 0} (\hat{g}_\epsilon^{(k+1)}(T_{k+}) + \check{g}_\epsilon^{(k+1)}(T_{k+}))}_{f^{(k+1)}(T_{k+})} \mathbf{R}^{(k+1)} \\ - \underbrace{\lim_{\epsilon \rightarrow 0} \frac{1}{\epsilon} (\hat{g}_\epsilon^{(k+1)}(T_{k+}) - \check{g}_\epsilon^{(k+1)}(T_{k+}))}_{-f'(k+1)(T_{k+})\sqrt{\mathbf{S}^{(k+1)}/2}} \sqrt{2\mathbf{S}^{(k+1)}},$$

which reproduces (30) for $0 < k < K$. Taking the difference of the two equations of (35) gives

$$0 = (\hat{g}_\epsilon^{(k)}(T_{k-}) - \check{g}_\epsilon^{(k)}(T_{k-}))\mathbf{R}^{(k)} + (\hat{g}_\epsilon^{(k)}(T_{k-}) + \check{g}_\epsilon^{(k)}(T_{k-}))\frac{1}{\epsilon}\sqrt{2\mathbf{S}^{(k)}} \\ - (\hat{g}_\epsilon^{(k+1)}(T_{k+}) - \check{g}_\epsilon^{(k+1)}(T_{k+}))\mathbf{R}^{(k+1)} - (\hat{g}_\epsilon^{(k+1)}(T_{k+}) + \check{g}_\epsilon^{(k+1)}(T_{k+}))\frac{1}{\epsilon}\sqrt{2\mathbf{S}^{(k+1)}},$$

which, multiplying by ϵ and decreasing ϵ to 0, provides the theorem.

Below we list the linear equations that provide the probability masses at the thresholds and the initial vectors of the matrix exponential terms of the density functions.

- Following the same pattern as in Section 3.2, for the lower (at T_0) and upper (at T_K) boundaries $2|\mathcal{S}| + |\mathcal{S}^{+(0)}| + |\mathcal{S}^{\sigma(0)}| + |\mathcal{S}^{-(K)}| + |\mathcal{S}^{\sigma(K)}|$ linear equations can be obtained.

– For the densities in region k ($0 < k < K$) we have (30), that is

$$\begin{aligned}
& p^{(k)} \tilde{\mathbf{Q}}^{(k)} \\
&= \underbrace{(\pi_f^{(k+1)} [\mathbf{I}\Psi_f^{(k+1)}] + \pi_b^{(k+1)} e^{\mathbf{K}_b^{(k+1)}(T_{k+1}-T_k)} [\Psi_b^{(k+1)} \mathbf{I}]) \mathbf{Z}^{(k+1)} \mathbf{R}^{(k+1)}}_{f^{(k+1)}(T_{k+})} \\
&- \underbrace{(\pi_f^{(k+1)} \mathbf{K}_f^{(k+1)} [\mathbf{I}\Psi_f^{(k+1)}] - \pi_b^{(k+1)} \mathbf{K}_b^{(k+1)} e^{\mathbf{K}_b^{(k+1)}(T_{k+1}-T_k)} [\Psi_b^{(k+1)} \mathbf{I}]) \mathbf{Z}^{(k+1)} \mathbf{S}^{(k+1)}}_{f'^{(k+1)}(T_{k+})} \\
&- \underbrace{(\pi_f^{(k)} e^{\mathbf{K}_f^{(k)}(T_k-T_{k-1})} [\mathbf{I}\Psi_f^{(k)}] + \pi_b^{(k)} [\Psi_b^{(k)} \mathbf{I}]) \mathbf{Z}^{(k)} \mathbf{R}^{(k)}}_{f^{(k)}(T_{k-})} \\
&+ \underbrace{(\pi_f^{(k)} \mathbf{K}_f^{(k)} e^{\mathbf{K}_f^{(k)}(T_k-T_{k-1})} [\mathbf{I}\Psi_f^{(k)}] - \pi_b^{(k)} \mathbf{K}_b^{(k)} [\Psi_b^{(k)} \mathbf{I}]) \mathbf{Z}^{(k)} \mathbf{S}^{(k)}}_{f'^{(k)}(T_{k-})},
\end{aligned} \tag{36}$$

providing $(K-1)|\mathcal{S}|$ further linear equations.

– Figure 1 lists all possible state combinations appearing at an internal threshold. The ones marked with $\boxed{}$ lead to probability mass accumulating at the threshold. For the rest of the states, however, we have that

$$p_i^{(k)} = 0. \tag{37}$$

The number of such states (and the related equations) is $|\mathcal{S}| - |\mathcal{S}^{0(k)}| - |\mathcal{S}^{0(k+1)}| + |\mathcal{S}^{0(k)} \cap \mathcal{S}^{0(k+1)}| - |\mathcal{S}^{+(k)} \cap \mathcal{S}^{-(k+1)}|$.

– If the threshold behavior in a given state falls into "Class 2" in Figure 1, then Theorem 2 applies, thus $f_i^{(k)}(T_{k-})\sqrt{s_i^{(k)}} = f_i^{(k+1)}(T_{k+})\sqrt{s_i^{(k+1)}}$. If the threshold behavior in a given state falls into "Class 3" or "Class 4" in Figure 1, then it will behave as an absorbing state: whenever the Brownian motion reaches the threshold, it stops there immediately, and the stationary density of the Brownian motion next to the threshold is zero. The neighbor regime either moves away the fluid level from the threshold (Class 3), or sticks the fluid level to the threshold (Class 4). Since in these cases the density at one side of the threshold and the the variance at the other side of the threshold are zero the boundary equation formally satisfies (32). As a result, for all of the "Class 2", "Class 3" and "Class 4" cases we have

$$\begin{aligned}
& \underbrace{(\pi_f^{(k)} e^{\mathbf{K}_f^{(k)}(T_k-T_{k-1})} [\mathbf{I}\Psi_f^{(k)}] + \pi_b^{(k)} [\Psi_b^{(k)} \mathbf{I}]) \mathbf{Z}^{(k)} \sqrt{\mathbf{S}^{(k)}}}_{f^{(k)}(T_{k-})} = \\
& \underbrace{(\pi_f^{(k+1)} [\mathbf{I}\Psi_f^{(k+1)}] + \pi_b^{(k+1)} e^{\mathbf{K}_b^{(k+1)}(T_{k+1}-T_k)} [\Psi_b^{(k+1)} \mathbf{I}]) \mathbf{Z}^{(k+1)} \sqrt{\mathbf{S}^{(k+1)}}}_{f^{(k+1)}(T_{k+})}.
\end{aligned} \tag{38}$$

It can be checked in Figure 1 that all states are affected except those where $\sigma_i = 0$ and $r_i > 0$ in the lower regime, those where $\sigma_i = 0$ and $r_i < 0$ in the upper regime, and the zero-zero transition (last case in "Class 1").

Therefore the number of equations is $|\mathcal{S}| - |\mathcal{S}^{+(k)}| - |\mathcal{S}^{-(k+1)}| + |\mathcal{S}^{+(k)} \cap \mathcal{S}^{-(k+1)}| - |\mathcal{S}^{0(k)} \cap \mathcal{S}^{0(k+1)}|$, which equals $-|\mathcal{S}| + |\mathcal{S}^{-(k)}| + |\mathcal{S}^{0(k)}| + |\mathcal{S}^{\sigma(k)}| + |\mathcal{S}^{+(k+1)}| + |\mathcal{S}^{0(k+1)}| + |\mathcal{S}^{\sigma(k+1)}| + |\mathcal{S}^{+(k)} \cap \mathcal{S}^{-(k+1)}| - |\mathcal{S}^{0(k)} \cap \mathcal{S}^{0(k+1)}|$.

- If the threshold behavior in a given state falls into "Class 5" in Figure 1, then it will behave as a reflecting state: whenever the Brownian motion crosses the threshold the other regime pushes it back, as in case of a reflecting boundary. There is no mass in these states, but there is a positive density next to the threshold.

Summing up the number of equations, from (37) and (38) we get $|\mathcal{S}^{-(k)}| + |\mathcal{S}^{\sigma(k)}| + |\mathcal{S}^{+(k+1)}| + |\mathcal{S}^{\sigma(k+1)}|$ equations for each internal threshold. The total number of equations is therefore $(K+1)|\mathcal{S}| + \sum_{k=1}^K |\mathcal{S}^{+(k)}| + \sum_{k=1}^K |\mathcal{S}^{-(k)}| + 2 \sum_{k=1}^K |\mathcal{S}^{\sigma(k)}|$, that matches the number of unknowns.

To make the linear set of equations full rank, the normalization condition has to be taken into consideration as well, hence equation

$$\begin{aligned} 1 = & \sum_{k=0}^K p^{(k)} \mathbb{1} + \sum_{k=1}^K \pi_f^{(k)} \int_0^{T_k - T_{k-1}} e^{\mathbf{K}_f^{(k)} x} dx \left[\mathbf{I} \Psi_f^{(k)} \right] \mathbf{Z}^{(k)} \mathbb{1} \\ & + \sum_{k=1}^K \pi_b^{(k)} \int_0^{T_k - T_{k-1}} e^{\mathbf{K}_b^{(k)} x} dx \left[\Psi_b^{(k)} \mathbf{I} \right] \mathbf{Z}^{(k)} \mathbb{1} \end{aligned}$$

has to be added. The integrals can be evaluated as in Section 3.2.

4.3 Infinite buffer case

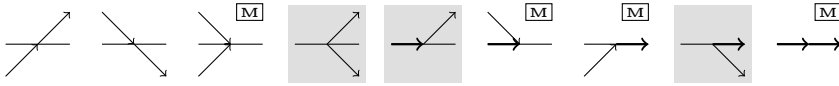
The level dependent infinite buffer second order Markov fluid model, thus $T_K = \infty$, can also be solved with slight modifications. For the stability of this model the drift in the last (infinite) regime should be negative. In this case the density function in the last regime consists of a single matrix-exponential term (with strictly negative eigenvalues like in (7)) instead of the matrix-exponential combination (like in (31)), but formally the solution can be obtained by replacing the linear equations related to the upper boundary with $p^{(K)} = 0$ and $\pi_b^{(K)} = 0$.

5 Numerical experiments

The presented procedures have been implemented in Matlab environment and are available to download¹. The implementation

¹ The implementation can be downloaded from <http://www.hit.bme.hu/~ghorvath/software>

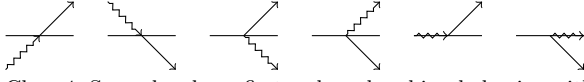
Class 1: First-order – first-order:



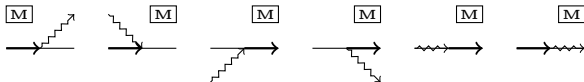
Class 2: Second-order – second-order:



Class 3: Second-order – first-order, absorbing behavior without mass:



Class 4: Second-order – first-order, absorbing behavior with mass:



Class 5: Second-order – first-order, reflexing behavior:

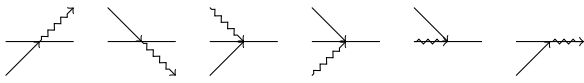


Fig. 1 All possible combinations of drift and variance changes at the internal threshold T_k . The arrows indicate the fluid behavior below and above the threshold. E.g., the last Class 5 pictogram refers to the case $r_i^{(k)} > 0, \sigma_i^{(k)} = 0, r_i^{(k+1)} = 0, \sigma_i^{(k)} > 0$ (the horizontal arrow is implicitly related with the upper region). The last two pictograms of Class 4 are interpreted from left to right and the last one refers to $r_i^{(k)} = 0, \sigma_i^{(k)} = 0, r_i^{(k+1)} = 0, \sigma_i^{(k)} > 0$.

uses the Cyclic Reduction algorithm of the SMCSolver toolbox [Bini et al(2006)Bini, Meini, Steffé, and Van Houdt] to solve the arising matrix quadratic equation.

5.1 Example of an ATM multiplexer from [Chen et al(2002)Chen, Hong, and Trivedi]

We first compute the stationary distribution of the example whose transient behaviour is studied in [Chen et al(2002)Chen, Hong, and Trivedi]. This example is related to a telecommunication application, to the analysis of an ATM multiplexer. The ATM multiplexer is fed by L independent, identical on-off sources. In the "on" state each source emits high priority ATM cells at rate λ_0 and low priority marked cells at rate λ_1 . If the buffer level is above a given threshold b , marked cells are dropped.

Most parameters are taken from [Chen et al(2002)Chen, Hong, and Trivedi]: The transition rate from "off" state to "on" state is 1, from "on" to "off" it is 0.4. The fluid rates are $\lambda_0 = 1$ Mbits/s and $\lambda_1 = 0.5$ Mbits/s. The service

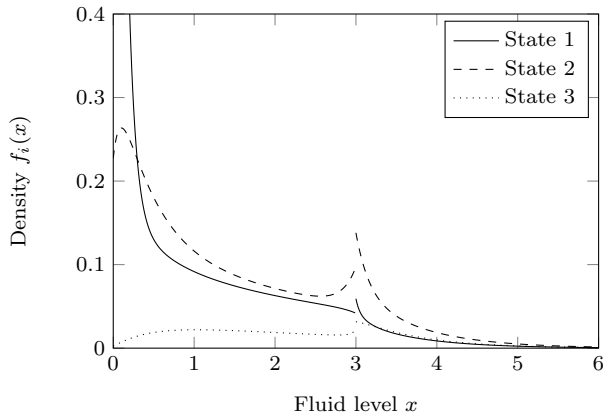


Fig. 2 State-dependent density function of the fluid level

capacity is $c = 1.1$ Mbits/s, hence the fluid rate matrices for $L = 2$ are

$$\mathbf{R}^{(1)} = \begin{bmatrix} -1.1 & & \\ & 0.4 & \\ & & 1.9 \end{bmatrix}, \quad \mathbf{R}^{(2)} = \begin{bmatrix} -1.1 & & \\ & -0.1 & \\ & & 0.9 \end{bmatrix}. \quad (39)$$

The buffer size b is 10 Mbits, while the threshold is set to 3 Mbits. The variances are 0.2 in all states below the threshold, and, different from [Chen et al(2002)Chen, Hong, and Trivedi], they are 0.1 above the threshold (in [Chen et al(2002)Chen, Hong, and Trivedi] the variances are level independent).

Figure 2 depicts the state dependent density function in case of $L = 2$. Since all states are second-order states in this example, the density function is non-zero around the threshold $b = 3$, but the discontinuity is clearly visible. It can also be observed that a considerable amount of probability is concentrated around the threshold in state 2, which is due to the fact that $r_2^{(1)} > 0$ and $r_2^{(2)} < 0$.

In the next experiment the variance matrices $\mathbf{S}^{(1)}$ and $\mathbf{S}^{(2)}$ are multiplied by a scaling factor and the mean queue length is investigated. The results are shown in Figure 3. As it is indicated by the plot the mean queue length increases with the variance significantly.

5.2 Scalability of the solution method

Next we investigate the scalability of the solution method. Figure 4 presents the execution time as the function of the number of states. The number of states is varied by the L parameter, thus the number of individual on-off sources feeding the queue. The computational bottleneck in this case is the solution of the matrix-quadratic equations providing the \mathbf{K} matrices. According to the results the algorithms used in SMCSolver toolbox are able to cope

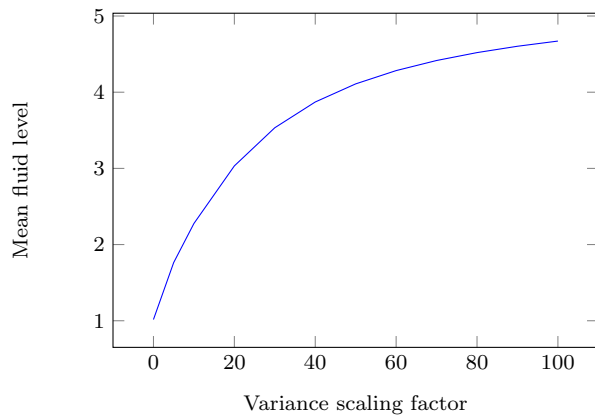


Fig. 3 The mean fluid level as the function of the variance

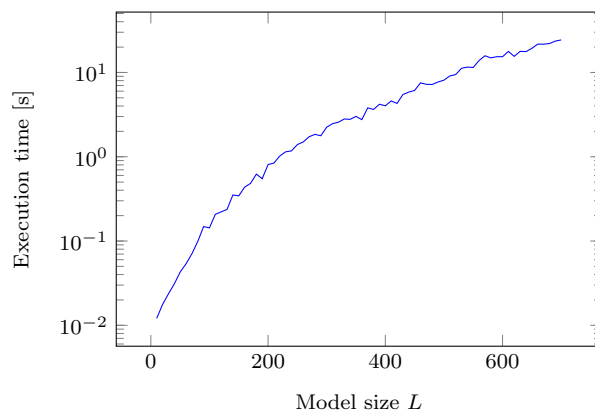


Fig. 4 Analysis time as the function of $|\mathcal{S}|$

with very large matrices in a couple of seconds as well. (The measurements have been made on an average PC with a CPU clocked at 3.4 GHz and 4 GB of memory.)

Finally, Figure 5 shows the execution time as the function of the number of thresholds. The model size is kept fixed, the background process consists of $L = 10$ on-off sources and we increase the number of equidistant thresholds. With a large number of thresholds the computational bottleneck is the solution of the linear system giving the masses and the initial vectors of the matrix-exponential densities.

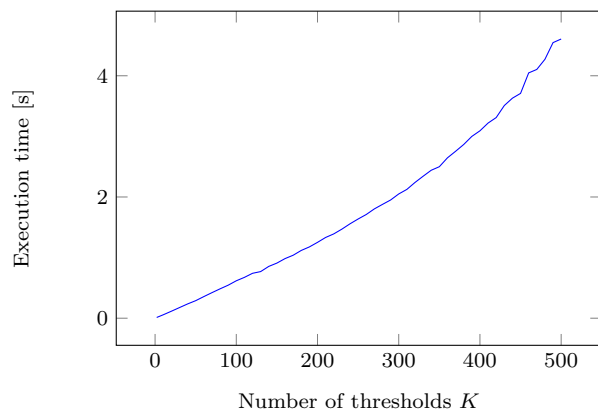


Fig. 5 Analysis time as the function of the number of thresholds

Acknowledgement

The authors thank the exceptional efforts of the anonymous reviewers. Their comments helped to improve the manuscript significantly. This research is partially supported by the OTKA-123914 project.

References

- [Ahn and Ramaswami(2017)] Ahn S, Ramaswami V (2017) A quadratically convergent algorithm for first passage time distributions in the markov-modulated brownian motion. *Stochastic Models* 33(1):59–96
- [Akar and Sohraby(1997)] Akar N, Sohraby K (1997) An invariant subspace approach in $M/G/1$ and $G/M/1$ type Markov chains. *Comm Statist Stochastic Models* 13(3):381–416
- [Akar and Sohraby(2004)] Akar N, Sohraby K (2004) Infinite-and finite-buffer Markov fluid queues: a unified analysis. *Journal of applied probability* pp 557–569
- [Asmussen(1995)] Asmussen S (1995) Stationary distributions for fluid flow models with or without Brownian noise. *Communications in statistics Stochastic models* 11(1):21–49
- [Bass and Pardoux(1987)] Bass RF, Pardoux E (1987) Uniqueness for diffusions with piecewise constant coefficients. *Probability Theory and Related Fields* 76(4):557–572, URL <https://doi.org/10.1007/BF00960074>
- [Bean and O'Reilly(2008)] Bean NG, O'Reilly MM (2008) Performance measures of a multi-layer markovian fluid model. *Annals of Operations Research* 160(1):99–120
- [Bekker et al(2009)] Bekker R, Boxma OJ, Resing JAC (2009) Levy processes with adaptable exponent. *Advances in Applied Probability* 41(1):117–205
- [Bini et al(2006)] Bini D, Meini B, Steffé S, Van Houdt B (2006) Structured Markov chains solver: software tools. In: *Proceeding from the 2006 workshop on Tools for solving structured Markov chains*, ACM, p 14
- [Bini et al(2005)] Bini DA, Latouche G, Meini B (2005) *Numerical Methods for Structured Markov Chains (Numerical Mathematics and Scientific Computation)*. Oxford University Press, Inc., New York, NY, USA
- [Breuer(2012)] Breuer L (2012) Exit problems for reflected markov-modulated brownian motion. *Journal of Applied Probability* 49(3):697–709

- [Chen et al(2002)Chen, Hong, and Trivedi] Chen D, Hong Y, Trivedi KS (2002) Second-order stochastic fluid models with fluid-dependent flow rates. *Performance Evaluation* 49(1):341–358
- [Cox and Miller(1972)] Cox DR, Miller HD (1972) *The theory of stochastic processes*. Chapman and Hall Ltd.
- [Gribaudo et al(2008)Gribaudo, Manini, Sericola, and Telek] Gribaudo M, Manini D, Sericola B, Telek M (2008) Second order fluid models with general boundary behaviour. *Annals of Operations Research* 160(1):69–82
- [Hohn et al(2004)Hohn, Veitch, Papagiannaki, and Diot] Hohn N, Veitch D, Papagiannaki K, Diot C (2004) Bridging router performance and queuing theory. *SIGMETRICS Perform Eval Rev* 32(1):355–366
- [Ivanovs(2010)] Ivanovs J (2010) Markov-modulated Brownian motion with two reflecting barriers. *Journal of Applied Probability* 47(4):1034–1047
- [Karandikar and Kulkarni(1995)] Karandikar RL, Kulkarni V (1995) Second-order fluid flow models: reflected brownian motion in a random environment. *Operations Research* 43:77–88
- [Latouche and Nguyen(2015a)] Latouche G, Nguyen G (2015a) Fluid approach to two-sided reflected Markov-modulated Brownian motion. *Queueing Systems* 80(1-2):105–125
- [Latouche and Nguyen(2015b)] Latouche G, Nguyen GT (2015b) The morphing of fluid queues into Markov-modulated Brownian motion. *Stochastic Systems* 5(1):62–86
- [Le et al(2007)Le, Aikat, Jeffay, and Smith] Le L, Aikat J, Jeffay K, Smith FD (2007) The effects of active queue management and explicit congestion notification on web performance. *IEEE/ACM Trans Netw* 15(6):1217–1230
- [Ramaswami(1999)] Ramaswami V (1999) Matrix analytic methods for stochastic fluid flows. In: *International Teletraffic Congress, Edinburg*, pp 1019–1030
- [Rogers(1994)] Rogers LCG (1994) Fluid models in queueing theory and wiener-hopf factorization of Markov chains. *The Annals of Applied Probability* 4(2):390–413
- [da Silva Soares and Latouche(2006)] da Silva Soares A, Latouche G (2006) Matrix-analytic methods for fluid queues with finite buffers. *Performance Evaluation* 63(45):295 – 314
- [da Silva Soares and Latouche(2009)] da Silva Soares A, Latouche G (2009) Fluid queues with level dependent evolution. *European J Oper Res* 196(3):1041–1048
- [Stanford et al(2005)Stanford, Latouche, Woolford, Boychuk, and Hunchak] Stanford DA, Latouche G, Woolford DG, Boychuk D, Hunchak A (2005) Erlangized fluid queues with application to uncontrolled fire perimeter. *Stochastic Models* 21(2-3):631–642, DOI 10.1081/STM-200056242
- [Stroock and Varadhan(2007)] Stroock DW, Varadhan SS (2007) *Multidimensional diffusion processes*. Springer
- [Telek and Vécsei(2012)] Telek M, Vécsei M (2012) Finite queues at the limit of saturation. In: *2012 Ninth International Conference on Quantitative Evaluation of Systems*, pp 33–42